van Hooff T, Blocken B. 2012. Full-scale measurements of indoor environmental conditions and natural ventilation in a large semi-enclosed stadium: possibilities and limitations for CFD validation. ***Journal of Wind Engineering and Industrial Aerodynamics*** 104-106: 330-341.

# Full-scale measurements of indoor environmental conditions and natural ventilation in a large semi-enclosed stadium: possibilities and limitations for CFD validation

T. van Hooff [a,b 1], B. Blocken [a]

[a]Building Physics and Services, Eindhoven University of Technology, P.O. Box 513, 5600 MB Eindhoven, The Netherlands.
[b]Division of Building Physics, Katholieke Universiteit Leuven, Kasteelpark Arenberg 40, P.O. Box 2447, 3001 Leuven, Belgium.

**Graphical abstract:**

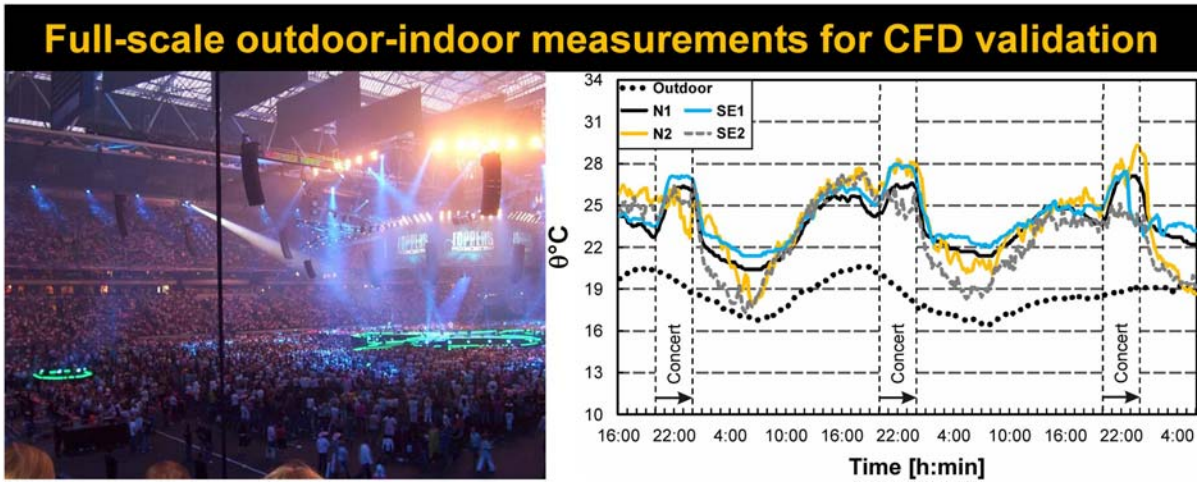


**Highlights:**

► Natural ventilation and indoor environmental conditions are important for energy, comfort and health in buildings.
► Accurate reduced-scale wind tunnel modeling is inhibited by similarity requirements.
► Therefore, full-scale on-site measurement data sets are needed for analysis and for CFD validation.
► This paper presents an extensive data set for the Amsterdam ArenA stadium, intended for CFD validation.
► Lack of repeatability is a known disadvantage of on-site measurements, but this is limited in this case.

[1] Corresponding author: E-mail address: t.a.j.v.hooff@tue.nl. Tel.: +31 (0) 40 247 5877; fax: +31 (0) 40 243 8595.

van Hooff T, Blocken B. 2012. Full-scale measurements of indoor environmental conditions and natural ventilation in a large semi-enclosed stadium: possibilities and limitations for CFD validation. ***Journal of Wind Engineering and Industrial Aerodynamics*** 104-106: 330-341.

# Full-scale measurements of indoor environmental conditions and natural ventilation in a large semi-enclosed stadium: possibilities and limitations for CFD validation

T. van Hooff [a,b 2], B. Blocken [a]

[a]Building Physics and Services, Eindhoven University of Technology, P.O. Box 513, 5600 MB Eindhoven, The Netherlands.
[b]Division of Building Physics, Katholieke Universiteit Leuven, Kasteelpark Arenberg 40, P.O. Box 2447, 3001 Leuven, Belgium.

**Abstract**

The use of Computational Fluid Dynamics (CFD) to study complex physical processes in the built environment requires model validation by means of reduced-scale or full-scale experimental data. CFD studies of natural ventilation of buildings in urban areas should be validated concerning both the wind flow pattern around the buildings and the indoor airflow driven by wind and buoyancy. Reduced-scale wind tunnel measurements and full-scale on-site measurements both have particular advantages and disadvantages. A main disadvantage of reduced-scale experiments is the difficulty to fulfill the similarity requirements, especially when wind flow and buoyancy effects are combined. This paper presents the results of unique full-scale measurements for a situation in which accurate wind tunnel experiments are not possible: natural ventilation and thermal, humidity and $CO_2$ concentration conditions inside a large semi-enclosed multifunctional stadium with relatively small ventilation openings. The emphasis is on three consecutive evenings on which concerts took place in the stadium. Although the repeatability of full-scale on-site measurements is in general quite low, nearly identical meteorological and indoor environmental conditions were present on the three concert evenings. Furthermore, the calculated air exchange rate based on $CO_2$ concentration decay measurements shows that also the natural ventilation on the three evenings was almost equal. The paper addresses the possibilities and limitations of this type of experimental data for the validation of CFD simulations. The data will be used in future studies for validation of CFD models for wind flow, natural ventilation and indoor environmental conditions in buildings.

*Keywords:* Full-scale measurements, urban area, indoor climate, air quality, natural ventilation, model validation, tracer gas decay, thermal comfort

## 1. Introduction

The use of numerical models requires model validation by means of reduced-scale or full-scale experimental data. In the past decades, an increasing amount of guidelines and papers have stipulated the importance of validation of numerical models in general, and of Computational Fluid Dynamics (CFD) in particular to ensure the trustworthiness of the simulation results (e.g. Schatzmann et al. 1997, Casey and Wintergerste 2000, Dalgliesh and Surry 2003, Franke et al. 2004, 2007, Tominaga et al. 2008, Schatzmann and Leitl 2011, Blocken et al. 2011, 2012, Blocken and Gualtieri 2012). The validation of numerical models that are used to analyze natural ventilation is not always straightforward. Numerical natural ventilation studies can use either a coupled or a decoupled approach, where the former consists of modeling the urban wind flow and the indoor air flow simultaneously and within the same computational domain (e.g. Kato et al. 1992, Jiang and Chen 2002, Evola and Popov 2006, Mochida et al. 2006, Hu et al. 2008, Norton et al. 2010, Kobayashi et al. 2010, van Hooff and Blocken 2010a, 2010b, Ramponi and Blocken 2012a, 2012b). Validation of these coupled models should focus on the wind flow pattern around the buildings as well as on the indoor airflow driven by wind and buoyancy. This requires high-quality experimental data, either from reduced-scale measurements in an Atmospheric Boundary Layer (ABL) wind tunnel, or by full-scale on-site measurements. The first has the advantage that the measurements are performed under controlled boundary conditions and have a strong degree of repeatability.

[2] Corresponding author: E-mail address: t.a.j.v.hooff@tue.nl. Tel.: +31 (0) 40 247 5877; fax: +31 (0) 40 243 8595.

On-site measurements on the other hand suffer from uncontrollable boundary conditions and lack of repeatability, due to the inherent variability of ABL meteorology (Schatzmann and Leitl 2011). Schatzmann et al. (1997) and Schatzmann and Leitl (2011) elaborated on the issues that are associated with the validation of CFD models for urban wind flow and dispersion simulations. The advantage of full-scale on-site measurements is that the real conditions are measured. In addition, many physical problems in wind engineering and building physics, such as wind-driven rain on buildings and heat and moisture transfer in porous building components require on-site measurements because these phenomena cannot (fully) be reproduced at reduced scale (e.g. Dalgliesh and Surry 2003, Blocken and Carmeliet 2005). The same holds for natural ventilation due to the combined effect of wind and buoyancy, as explained below.

Natural ventilation can be driven by wind and/or buoyancy (e.g. Linden 1999, Hunt and Linden 1999, Li and Delsante 2001, Heiselberg et al. 2004). For buoyancy-driven ventilation of buildings, the representation of the indoor thermal conditions and the vapor concentration is very important. Reduced-scale measurements can be deficient to reproduce these conditions, as pointed out by among others Chen (2009), since these measurements can suffer from scaling problems associated with the combined modeling of inertial and buoyancy forces. For the inertial forces the Reynolds number should be the same, or at least high enough to ensure a fully turbulent flow field which is Re-independent. This holds for the building Reynolds number as well as for the Reynolds number of the ventilation openings. Ruck (1993) recommends a building Reynolds number of at least 10,000 for wind tunnel measurements of ABL flow. Special attention however should be given to the ventilation flow through relatively small openings in the building facade, which might lead to Reynolds number effects due to the reduced length scale in the wind tunnel. A too large reduction of the opening size might lead to either transitional or laminar flow through the model-scale openings, instead of turbulent flow. In addition, reduced-scale measurements including thermal effects require similarity of the Grashof and Richardson numbers. The Grashof number is given by:

$$Gr = \frac{\beta g H^3 \left( T_w - T_{ref} \right)}{\nu^2} \tag{1}$$

with β the thermal expansion coefficient ($K^{-1}$), g the gravitational acceleration (= 9.81 $m/s^2$), H the height of the building, $T_w$ the average wall temperature (K) and $T_{ref}$ the average reference temperature (K). Grashof numbers above $10^9$ indicate turbulent convection close to the heated surface, whereas values lower than $10^8$ indicate laminar convection (Bejan 1984, Ruck 1993). In addition to the Grashof number, one should also consider the Richardson number, which represents the importance of natural convection compared to forced convection, and which is defined as $Ri = Gr/Re^2$. The Richardson number is equal to the inverse Froude number (1/Fr). When $Ri \approx 1$, thermal and mechanical effects are equally important, whereas for $Ri >> 1$ thermal effects dominate the flow. Note that the similarity requirement for Ri is automatically fulfilled when both Re and Gr for the reduced-scale experiments are equal to the full-scale values. However this is not always the case; e.g. the Re values in the wind tunnel are often several orders of magnitude smaller than in reality. As a result of these similarity requirements, the collection of a proper set of experimental validation data for numerical models dealing with non-isothermal natural ventilation studies is far from straightforward.

In literature, several studies can be found that describe wind tunnel measurements that include thermal effects. Ruck (1993) studied the airflow around a heated cubic building model in the wind tunnel. From his measurements it was concluded that the reattachment length altered significantly, starting from a Richardson number of about 0.2. Kovar-Panskus et al. (2002) studied the influence of solar radiation on the flow pattern in a 2D urban street canyon. Their measurements were conducted for Froude numbers in the range 0.27 to 2 and also indicated the influence of the heated building surfaces on the flow pattern inside the urban street canyon. Richards et al. (2006) performed wind tunnel measurements of wind flow around an isolated building with a heated leeward wall. They stated that it was almost impossible to fulfill all similarity requirements and therefore decided not to replicate typical full-scale conditions but to model the scaled conditions for mixed and forced convection. The vast majority of reduced-scale natural ventilation studies in ABL wind tunnels were performed for isothermal conditions, e.g. Kato et al. (1992), Straw et al. (2000), Ohba et al. (2001), Jiang et al. (2003), Karava et al. (2007, 2011), Kobayashi et al. (2010), whereas experimental studies on natural ventilation including thermal effects are often conducted without the effects of ABL wind flow, e.g. Holford and Hunt (2003), Liu et al. (2009).

An example of a study in which the natural ventilation needs to be assessed is that of the Amsterdam ArenA (Fig. 1) multifunctional stadium in the Netherlands. For this stadium with its very large indoor volume of 1.2 x $10^6$ $m^3$, natural ventilation is important to ensure a comfortable and healthy indoor environment. A previous study by van Hooff and Blocken (2010b) has indicated the necessity of explicitly modeling the urban surroundings of the stadium in order to obtain accurate natural ventilation rates. The urban area that was taken into account in their study was about 700 x 700 $m^2$. The modeling scale for this area, in a typical ABL wind tunnel with a cross-section of 2 x 2 $m^2$, would then be at least 1:500. For a 1:500 scale model, the minimum

building Reynolds numbers for a wind tunnel experiment are still achievable without too much effort; the building Reynolds number already surpasses the critical value of 10,000 for low reference velocities of 1.2 m/s. However, at this scale the dimensions of the smallest ventilation openings (full-scale size = 0.2 m) would be around $4.10^{-4}$ m (= 0.4 mm), which implies that the resulting Reynolds numbers through these openings, based on a relatively high characteristic velocity of 5 m/s, would be around 128 (full-scale value around 64,000). In addition to the fact that an opening of 0.4 mm cannot be properly made in a wind tunnel model, the flow through such opening would be laminar and not representative of the actual turbulent flow.

For non-isothermal reduced-scale experiments one should also fulfill the similarity requirements associated with thermal modeling, as indicated above. Based on the building height (H) of 70 m and a temperature difference inside the stadium ($T_w$-$T_{ref}$) of 10°C, the Grashof number for full-scale conditions becomes larger than $10^{14}$, indicating turbulent convection. The Grashof number for the reduced-scale measurements should therefore be at least $10^9$ to measure turbulent convection. However, due to the scale of the model (1:500), which is fixed due to the large area of interest, it would require unrealistically high temperature differences of at least 2,800 K (!) to measure at Gr-numbers above $10^9$. An extra problem would be the changing air density when the temperatures become very large, as indicated by Richards et al. (2006). In addition to the similarity requirements for the Reynolds number and the Grashof number, one should also make sure that the Richardson number is similar to the full-scale conditions in order to measure at the correct balance between natural convection and forced convection.

Given the large difficulties in obtaining reliable reduced-scale data, this paper presents unique full-scale on-site measurement data of natural ventilation and indoor environmental conditions in the large semi-enclosed ArenA stadium. The experiments were performed to provide experimental data for CFD validation. The paper also discusses the possibilities and limitations of this type of full-scale data. First, a description of the stadium is given in Section 2. Second, the experimental set-up is described in section 3. Next, in section 4, the measurement results are presented. Finally, sections 5 (discussion) and 6 (conclusions) conclude the paper.

## 2. Description of stadium and surroundings

### 2.1 Surroundings

The Amsterdam ArenA stadium (Fig. 1) is located in the southeast area of Amsterdam. The city and its surroundings are located on very flat terrain; topographical height differences are limited to less than 6 m. This area of Amsterdam is still under development, and several new large and high-rise buildings are planned in the vicinity. The height of the current surrounding buildings varies from 12 m to a maximum of 95 m for the "ABN-AMRO" office building (see Fig. 1a). The aerodynamic roughness length $y_0$ of the surroundings is determined based on the updated Davenport roughness classification (Fig. 2) (Wieringa 1992). The area on the north side of the ArenA can be classified as "closed terrain" due to the urban character that is present in a radius of 10 km upwind. The estimated $y_0$ for this area is 1.0 m. The south side area of the ArenA is not as rough as the north side due to the presence of agricultural and natural areas and can be characterized with an $y_0$ of 0.5 m.

### 2.2 Stadium

The ArenA is a so-called oval stadium with a dome-shaped roof. Figures 3a-c show a detailed plan view and two vertical cross-sections αα' and ββ'. The exterior stadium dimensions are 226 x 190 x 72 $m^3$ (L x W x H) and the interior volume is about 1.2 x $10^6$ $m^3$. The stands consist of two separate concrete tiers, which run along the entire perimeter of the stadium. The roof consists of a steel roof construction, which is largely covered with semi-transparent polycarbonate sheets, while steel sheets are applied near the gutter. Fig. 4a shows a cross-section of the stadium, in which different components can be distinguished, indicated with numbers. Numbers 1 and 2 are the logistic rings in which facilities and the entrances to the interior stadium volume are situated. Number 3 is an elevated circulation deck that runs around the stadium. It serves as parking and logistics area and is known as the *ArenA deck*. Four large gates in the corners of the stadium (Fig. 3a, 4b) connect the ArenA deck (Fig. 4a) with the stadium interior. Each gate has a cross-section $L_g$ x $H_g$ = 6.2 x 6.7 $m^2$ and can be individually opened and closed. Number 4 indicates a safety and facility ring that separates the stands from the pitch. This ring runs along the entire perimeter of the field and connects the four gates. The parking deck under the stadium is indicated with number 5.

In absence of Heating, Ventilation, and Air-Conditioning (HVAC) systems, natural ventilation is the only means to ensure indoor air quality. Natural ventilation can occur through the openings that are present in the stadium envelope. The roof is the largest potential opening (4,400 $m^2$). However, during concerts and other festivities, which are usually held in the summer period, the roof is closed most of the time to provide shelter from rain and wind for the spectators and the technical equipment. When the roof is closed, natural ventilation of the stadium can only occur through a few smaller openings. The four gates in the corners of the stadium form

the second largest (potential) opening (4 x 41.5 $m^2$) (Fig. 3a and 4b). Additionally, two relatively narrow openings are present in the upper part of the stadium. The first narrow opening with a surface area of 130 $m^2$, is situated between the stand and the steel roof construction and runs along the entire perimeter of the roof (Fig. 4c). The second narrow opening is situated between the fixed and movable part of the roof (Fig. 4d). This opening is only present along the two longest edges of the stadium and has a total surface area of about 85 $m^2$.

## 3. Description of experimental set-ups

Experimental data for natural ventilation of the ArenA stadium should include information on the outdoor meteorological conditions, including the wind-flow pattern around the stadium, as well as information on the indoor environmental conditions. Two sets of measurements were conducted. The first set consisted of measurements of outdoor and indoor environmental conditions from the end of May until September 2007, with specific focus on three consecutive days on which concerts were held inside the stadium, because of the special indoor conditions during the concerts. The second set consisted of wind velocity measurements around the stadium and in the gates (openings) during days with high wind speeds and negligible thermal effects. This data set can be used for validation of CFD simulations of the isothermal wind-flow pattern around the stadium. These measurements were conducted from September to November 2007. Note that the wind measurements were not conducted simultaneously with the measurements of the indoor environmental conditions.

### *3.1 Indoor environmental conditions and natural ventilation*

The measurements to assess the indoor environmental conditions and the natural ventilation were conducted at four positions inside the stadium; two in the upper part of the first tier (N1, SE1), and two in the upper part of the second tier (N2, SE2) (Fig. 5a,b). The number of indoor measurement positions was limited to four due to practical and financial constraints. The four measurement units are placed in the northwest part of the stadium (N1, N2), and the southeast part of the stadium (SE1, SE2). The locations of the measurement set-ups were chosen in such a way that possible differences due to solar irradiation (N vs. SE) and due to possible thermal stratification (first tier vs. second tier) inside the stadium could be detected. Furthermore, the risk of vandalism by concert spectators was minimized by positioning the measurement set-ups sufficiently high (> 3 m) above the stands. Each measurement unit consisted of sensors to monitor the air temperature, relative humidity, globe temperature, air speed and $CO_2$ concentration. All variables were measured once per minute and saved to data loggers that were installed as part of each measurement unit.

#### *3.1.1 Solar radiation, temperature, indoor air speed and relative humidity*

To assess the influence of solar irradiation on the indoor air temperature, measurements were performed using a pyranometer, which was installed in the gutter of the stadium. The pyranometer of Kipp & Zonen (type CM11) is capable of measuring irradiation flux E within a range of 0-1400 W/$m^2$, with an expected error in the hourly radiation totals of 3% (Kipp and Zonen 2000).

The measurements of indoor air temperature ($\theta_a$) were conducted at the four positions described above. The air temperature was measured using sensors by Escort, type Junior EJ-HS. These sensors measure the air temperature with an accuracy of ±0.3˚C. The reference outdoor air temperature was measured simultaneously at the position at the ArenA-deck (Fig. 5b). In addition to the measurements of air temperature, the globe temperature ($\theta_g$) was measured using a black-globe thermometer. The mean radiant temperature ($\theta_{MRT}$) can be calculated from $\theta_g$ and the indoor air speed v (in m/s) using Equation 2 (McIntyre 1980) in case $\theta_a \approx \theta_{MRT}$. It is defined as the area weighted mean temperature of all the objects surrounding the body. The mean radiant temperature is among others used in thermal comfort studies.

$$\theta_{MRT} = \theta_g + 2,44\sqrt{v}\left(\theta_g - \theta_a\right) \qquad (2)$$

The indoor air speed was also measured at the four indoor positions, with hot-sphere anemometers of the type Sensor HT-412-2, with an accuracy of 0.02 m/s in the range of 0.05-1 m/s.

Finally, the relative humidity was also measured at the four indoor positions and the outdoor position with the Escort type Junior EJ-HS sensors, with an accuracy of ±3%. The water vapor concentration ($x_v$) can be obtained by using Equations 3 (WMO 2008) and 4 (Awbi 2007), in which the measured air temperature and the relative humidity are inserted:

$$p_{v;sat} = 611.2 \cdot \exp\left(\frac{17.62\theta_a}{243.12 + \theta_a}\right) \quad (3)$$

$$x_v = \frac{0.622\, p_v}{101325 - p_v} \cdot 1000 = \frac{0.622\, p_{v;sat} \cdot RH}{101325 - p_{v;sat} \cdot RH} \cdot 1000 \quad (4)$$

with $p_{v;sat}$ the saturated water vapor pressure and $p_v$ the water vapor pressure.

#### *3.1.2 $CO_2$ concentration*

The natural ventilation of an enclosure can be assessed by performing tracer gas measurements (Lagus and Persily 1985, Sherman 1990). Based on these concentration measurements one can determine the air exchange rate (ACH – Air Changes per Hour). One of the most frequently used methods is the concentration decay method. It consists of filling the enclosure with a tracer gas until a uniform concentration is present in the entire enclosure, after which the decay of the tracer gas due to the ventilation can be used to calculate the ACH value. In this study $CO_2$ concentration is used as a tracer gas. During the concerts, the spectators are the $CO_2$ source, and the $CO_2$ concentration reaches a maximum at the end of the concert. After the spectators have left the stadium, the $CO_2$ concentration decreases due to natural ventilation, until it reaches the outdoor concentration. As such, these concerts provide a very suitable opportunity to measure the natural ventilation of the stadium, at a time when its indoor environment is used most intensively. The $CO_2$ values are measured at the four previously mentioned indoor positions, using $CO_2$ concentration sensors of Vaisala and SenseAir, both with a range of 0-2000 ppm. The ACH can be determined using Equation 5 (ASHRAE 2005):

$$ACH = \frac{\ln(c_0) - \ln(c_1)}{\tau_1 - \tau_0} \quad (5)$$

where ACH is the air exchange rate in $h^{-1}$, $C(\tau_0)$ is the concentration at time 0 in ppm, $C(\tau_1)$ the concentration at $\tau_1$ in ppm and $(\tau_1-\tau_0)$ the time between the two measurements.

### *3.2 Wind velocity measurements*

Measurements of the 3D wind velocity vector around the stadium were performed on days with high reference wind speeds ($U_{ref}$ > 8 m/s), in an attempt to focus on situations with neutral stratification. The reference wind velocity $U_{ref}$ was measured using an ultrasonic anemometer on a 10 m high post on top of the 95 m high ABN-AMRO office tower (Fig. 1a). The other measurements were conducted using ultrasonic anemometers on mobile posts, enabling the collection of measurement data on a variety of positions on the stadium deck, and in the gates. The measurement frequency was 5 Hz, after which the measurements were averaged into 10-min values and analyzed. Only data with at least 12 different 10-min values per reference wind direction sector of 10° were used. From these measurements, amplification factors $U/U_{ref}$ were derived, which can be used for the validation of isothermal simulations, as described by Blocken and Persoon (2009) and van Hooff and Blocken (2010a, 2010b). Note that these measurements were conducted from September-November 2007, and thus not simultaneously with the measurements of the indoor environmental conditions and natural ventilation.

## 4. Measurement results

First, the measurements of the environmental conditions and the $CO_2$ concentration are shown and discussed, with specific emphasis on three consecutive evenings in the beginning of June 2007 on which three similar concerts were held and on which the roof was closed. Second, the results of the wind velocity measurements are briefly addressed.

### *4.1 Indoor environmental conditions and natural ventilation*

#### *4.1.1 Solar radiation, temperatures, indoor air speed and water vapor pressure*

Although the use of solar irradiation levels is uncommon in CFD simulations of natural ventilation, the measurement results can be used to validate other thermal simulations (e.g. building performance simulations).

Figure 6 shows the measured irradiance of the sky E and the measured air temperature $\theta_a$ inside (position N2) and outside the stadium on both a sunny day (July 18) and a cloudy day (July 20). Note that the roof was closed, but no concerts took place during the irradiance measurements presented in this subsection, enabling an assessment of solely the influence of solar irradiation. It is shown that the indoor air temperature was up to 6°C higher than the outdoor temperature on the sunny day. This temperature difference was the result of the combined effect of incoming solar radiation through the semi-transparent polycarbonate sheets of the roof and of insufficient natural ventilation. Note that the polycarbonate sheets allow the entrance of short-wave radiation, which is subsequently absorbed by the stadium interior surfaces, but that it blocks the passage of the long-wave radiation that is emitted by the stadium interior surfaces (i.e. the greenhouse effect). On the cloudy day, the indoor air temperature was only up to 3°C higher than the outdoor air temperature.

Figure 7 shows the measured outdoor air temperature and the indoor air temperature at the four positions inside the stadium on three consecutive concert evenings. The outdoor air temperature at the end of the concert, at 24:00, and thus at the beginning of the $CO_2$ decay measurements, was around 19°C, 17.5°C and 19°C on June 1, June 2 and June 3 respectively, while the indoor air temperatures were significantly higher and also showed considerable variation between the different positions, indicating strong temperature gradients inside the stadium. Due to the presence of the spectators, the indoor air temperature rose up to about 10° higher than the outdoor air temperature. Note that the air temperatures at N2 and SE2 were in general lower during the night, which was most probably caused by the fact that they were located in the direct vicinity of the ventilation openings near the roof gutter. Finally, the influence of the approximately 50,000 spectators on the air temperature is clearly visible; the air temperature clearly rose from the beginning of the concerts at 20:00 hours with about 2-4°C, and decreased after 0:00 hours, when the spectators had left the stadium.

The globe temperature can be used to determine the mean radiant temperature which can be used in thermal comfort predictions and gives an area weighted mean temperature of all the objects surrounding the globe thermometer. Figure 8a shows that the difference between the measured air temperatures ($\theta_a$) and globe temperatures ($\theta_g$) at position N2 was small, and therefore the use of Equation 2 was justified. To calculate the mean radiant temperature with this equation, the air velocity is needed. The air speed for the given measurement period on June 2 fluctuated around 0.12 m/s (Fig. 8b). The resulting mean radiant temperature is depicted in Figure 8c, illustrating the lower value of $\theta_{MRT}$ compared to $\theta_a$. However, the difference is less than 2°C for this measurement period. This small difference between the air temperature and the mean radiant temperature indicates the absence of surfaces with a high surface temperature. This is attributed due to the lack of direct insolation of the stadium interior surfaces, due to the closed roof.

Figure 9 shows the water vapor concentration, $x_v$, outdoor as well as at the four indoor measurement positions, from the afternoon of June 1 until the morning of June 4. Except during and after the concert evenings, the value of $x_v$ was around 7-11 g/kg, and the values at the outdoor measurement position and the indoor positions do not show large differences. However, during the concerts the indoor water vapor concentration increased to 12-16 g/kg as a result of the moisture production by the spectators. Note that the four measurement positions again show considerable differences, illustrating concentration gradients inside the stadium. Based on an ACH of 0.67 $h^{-1}$ (which is the value determined by the $CO_2$ measurements in the next section), 50,000 spectators and a time interval of four hours, the water vapor emission rate per person would then be around 100 g/h. Note that this value lies between the values for a person in rest (50 g/h) and a person performing a low level of physical exercise (200 g/h) (ECA 1992).

### *4.1.2 Natural ventilation*

The measured $CO_2$ concentration decay curves at the four indoor measurement positions on the evening and night of June 2-3 are depicted in Figure 10. The period of interest is between 24:00 and about 2:00, which is the time between the end of the concert and removal of the $CO_2$ sources/spectators, and the time at which the indoor $CO_2$ concentration had reached the level of the outdoor concentration. The natural logarithms of the $CO_2$ concentrations are shown on the vertical axis and the decay is illustrated with the straight black lines, which have approximately the same slope, indicating relatively small deviations between the values of ACH for the four positions on this particular evening. Furthermore, it is worth mentioning that the fluctuations of the $CO_2$ concentration at positions N2 and SE2 were larger than at N1 and SE1. The most probable reason for this difference is the fact that positions N2 and SE2 are located in the direct vicinity of the ventilation opening between the stand and the steel roof construction (see Fig. 5b). This results in a higher unsteadiness of the $CO_2$ concentrations due to the exchange of indoor air with less polluted outdoor air through this ventilation opening.

The $CO_2$ concentration decay curves on three consecutive evenings (June 1 – June 3) are overlaid on each other in Figure 11. It can again be seen that the fluctuations at position N1 were smaller than at SE2, as described above. Furthermore, it can be noted that the decay curves on the three consecutive evenings are quite similar, especially at position N1. Table 1 shows the calculated ACH values for the three consecutive evenings based on the decay curves of $CO_2$ concentration. Note that the $CO_2$ concentration measurement at point SE1 on

June 3-4 failed due to equipment malfunctioning. Although differences are present between the four measurement positions, and also between the three consecutive evenings, the total average ACH was around 0.67 $h^{-1}$ with a relatively small maximum deviation of about ±10% for the values at each individual position. The ACH values based on the $CO_2$ concentration decay curves on three consecutive evenings were within 8% of the average ACH value for each particular position. This – albeit limited – indication of repeatability provides confidence in using these measurement data for the validation of numerical simulation models.

### *4.2 Wind velocity*

During the measurements of natural ventilation and indoor environmental conditions, the set-up of ultrasonic anemometers described in section 3.2 was not yet operational. Instead, measurement data from the meteorological station at Schiphol airport of the KNMI (Royal Meteorological Institute of the Netherlands) were used for this period. The hourly averaged wind speed $U_{10}$ measured by the KNMI at Schiphol Airport on these three evenings was about 2-3 m/s and the wind direction on all three days was about 30-50° from north (see Fig. 12).

The wind velocity measurements were conducted during autumn of 2007, on days with high measured reference wind speeds ($U_{ref}$ > 8 m/s). During these days thermal effects were negligible and therefore these measurements could be used to perform an isothermal validation of the wind flow around the stadium using a CFD model. Blocken and Persoon (2009) and van Hooff and Blocken (2010a, 2010b) elaborated on the measurement results, these are therefore not repeated in the present paper.

## 5. Discussion

The discussion focuses on four issues: (1) the advantages and disadvantages of full-scale on-site measurements versus reduced-scale wind tunnel measurements; (2) the limited number of measurement positions inside the stadium; (3) the repeatability of the full-scale measurements; and (4) the possibilities and limitations of the full-scale measurements for CFD validation.

### *5.1. Full-scale on-site measurements versus reduced-scale wind tunnel measurements*

Full-scale on-site measurements and reduced-scale wind tunnel measurements both have particular advantages and disadvantages. In wind tunnel measurements, the boundary conditions can be accurately controlled and the repeatability of the measurements is very high. However, for reproducing natural ventilation and indoor environmental conditions in buildings, reduced-scale wind tunnel measurements have several important disadvantages. First, it is generally very difficult or impossible to satisfy the similarity requirements in case of non-isothermal conditions (in terms of Reynolds, Grashof and Richardson number). In addition, for buildings with relatively small ventilation openings that are situated in urban areas, large wind tunnel scaling factors are required, which can lead to model-scale ventilation openings that become so small that the flow through them will be laminar or transitional, rather than turbulent. In such cases, full-scale measurements are required for model validation. The main advantages of full-scale on-site measurements are the measurement of the real conditions and the absence of scaling problems. Apart from model validation purposes, full-scale measurements can also be very useful to obtain insight in the physical processes related to natural ventilation and indoor environmental conditions in buildings.

This paper is focused on a situation in which accurate reduced-scale wind tunnel experiments are not possible: natural ventilation and thermal, humidity and $CO_2$ concentration conditions inside a large semi-enclosed multifunctional stadium with relatively small ventilation openings. However, known disadvantages of full-scale measurements in the real atmospheric boundary layer are (1) the limited number of measurement positions and (2) the uncontrollable boundary conditions and the variability (and lack of repeatability) of the measurements due to the inherently unsteady meteorological conditions (Schatzmann et al. 1997, Schatzmann and Leitl 2011). These two limitations are addressed in sections 5.2 and 5.3.

### *5.2. Limited number of measurement positions inside the stadium*

Indoor measurements of temperatures, indoor air speed, relative humidity and $CO_2$ concentration were only conducted at four positions. The number of positions was limited due to practical and financial constraints. However, the locations of these four measurement units were selected carefully, in such a way that possible differences due to solar irradiation (N vs. SE) and due to possible thermal stratification (first tier vs. second tier) inside the stadium could be detected. The measurement results indeed showed considerable variations in the measured environmental parameters between the different positions, indicating significant gradients of these parameters inside the stadium. As an example, the fluctuations of the $CO_2$ concentration at positions N2 and

SE2 were larger than at N1 and SE1. The most probable reason for this difference is the fact that positions N2 and SE2 are located in the direct vicinity of the ventilation opening between the stand and the steel roof construction (see Fig. 5b). This results in a higher unsteadiness of the $CO_2$ concentrations due to the exchange of indoor air with less polluted outdoor air through this ventilation opening. Given the differences in indoor environmental parameters measured at the four positions, it is clear that additional measurement positions would have further increased the value of the data set. On the other hand, it is important to mention that on-site full-scale experimental data of the type presented in this study are very rare, and are therefore considered to be very valuable. It should be noted that, although the $CO_2$ concentration decay curves show some differences among the four measurement positions, there is only a relatively small maximum deviation in ACH of about ±10% for the values at each individual position (from the total average ACH of about 0.67 $h^{-1}$). Therefore, the ACH values were approximately the same at the four measuring positions, providing confidence in the use of this - albeit spatially limited - data set to validate CFD simulations of natural ventilation of the stadium.

### *5.3. Repeatability of the full-scale measurements*

Known disadvantages of on-site measurements are the uncontrollable boundary conditions and lack of repeatability, due to the inherent variability of the ABL meteorological conditions (Schatzmann and Leitl 2011). In this paper, the measurements of the indoor environmental conditions were mainly focused on three consecutive concert evenings in the stadium. Figures 7, 9 and 10 show a fairly high degree of repeatability in terms of indoor and outdoor air temperature, indoor and outdoor water vapor concentration and indoor $CO_2$ concentration. In addition, Figure 12 also shows that the outdoor reference wind speed and wind direction were quite similar during all three concert evenings. The ACH values based on the $CO_2$ concentration decay curves on three consecutive evenings are within 8% of the average ACH value for each particular position. This indicates a fairly high degree of repeatability, for at least the three concerts evenings that were part of the measurements.

### *5.4. Possibilities and limitations of the full-scale measurements for CFD validation*

Throughout this paper, several possibilities and limitations of the full-scale measurements for CFD validation have been mentioned and discussed. This subsection provides a summary of the specific possibilities and limitations of the full-scale measurements presented in this paper. The following main possibilities and advantages of these data for CFD validation are noted:

- The full-scale measurements do not violate similarity constraints, and provide real and realistic data on natural ventilation due to the combined effect of wind and buoyancy, which could not have been obtained with reduced-scale wind tunnel measurements.
- The measurements at four different indoor positions allow validation of the reproduction of spatial gradients by the CFD models.
- The simultaneous measurement of many parameters (outdoor and indoor air temperature, water vapor concentration, $CO_2$ concentration, solar radiation and reference wind speed and wind direction) allow validation of the combined processes of heat and mass transfer inside the stadium.
- The measurements on the three concert evenings show a fairly high degree of repeatability, which benefits their use for CFD validation.
- The use of the spectators as $CO_2$ sources and the use of the concentration decay method after concerts is a rather unique approach to determine the air exchange rate of the stadium indoor environment.

The two main limitations and disadvantages of these data for CFD validation are:

- The limited number of indoor measurement positions
- The limited number of concert evenings over which measurement data can be averaged to reduce the uncertainty due to the inherent meteorological variability.

Note that the quite large differences in temperature, water vapor concentration and $CO_2$ concentration that were measured at the four different indoor measurement positions suggest that numerical modeling of the natural ventilation and indoor environmental conditions should be performed by advanced numerical models such as CFD, rather than by simplified models that assume that the indoor temperature and concentration distributions are uniform in the stadium interior. For an overview of the complete range of existing ventilation models, the reader is referred to the work by Chen (2009).

## 6. Summary and conclusions

The use of Computational Fluid Dynamics (CFD) to study complex physical processes in the built environment requires model validation by means of reduced-scale or full-scale experimental data. CFD studies of natural ventilation of buildings in urban areas should be validated concerning both the wind flow pattern around the buildings and the indoor airflow driven by wind and buoyancy. This paper has presented the results of unique on-site full-scale measurements for a situation in which accurate reduced-scale wind tunnel experiments were not possible: natural ventilation and thermal, humidity and $CO_2$ concentration conditions inside a large semi-enclosed multifunctional stadium with relatively small ventilation openings. Two sets of measurements were conducted. The first set consisted of measurements of outdoor and indoor environmental conditions from the end of May until September 2007, with specific focus on three consecutive days on which concerts were held inside the stadium, because of the special indoor conditions during the concerts. The stadium roof was closed during this period to protect equipment and spectators from wind and rain. Measurements were conducted of solar irradiation, air temperature, globe temperature, air speed, relative humidity and $CO_2$ concentration. The measurements took place on four different positions inside the semi-enclosed stadium, and the reference air temperature and relative humidity were measured simultaneously outside the stadium. The concentration decay method was used to determine the air exchange rate by natural ventilation.

The second set consisted of wind velocity measurements around the stadium and in the gates (openings) during days with high wind speed and negligible thermal effects. This data set can be used for validation of CFD simulations of the isothermal wind-flow pattern around the stadium. These measurements were conducted from September to November 2007.

The presented measurement data, especially during the concert evenings, are quite unique and are considered valuable for CFD validation, for several main reasons:

- Full-scale on-site simultaneous measurements of a wide range of indoor environmental parameters are scarce.
- The concerts in the stadium provide strong temporal variations in indoor environmental parameters, which in turn provides a challenging case for validation of transient CFD modeling.
- The use of the spectators as $CO_2$ sources and the use of the concentration decay method is a rather unique approach to determine the air exchange rate of the stadium indoor environment.
- Although the repeatability of full-scale on-site measurements is in general quite low, nearly identical meteorological and indoor environmental conditions were present on the three concert evenings. This is an important observation, given the importance of repeatability in order for the data to be suitable for validation purposes.

From the measurement data, the following additional conclusions can be made:

- On a typical sunny day, the irradiation of the sky had a strong influence on the indoor air temperature for the stadium with closed roof. The temperature difference between the indoor air and the outdoor air easily rose up to 6°C. On a typical cloudy day, this difference was only 2-3°C.
- During the concerts, the indoor air temperature increased significantly up to a maximum difference of 10°C compared to the outdoor air temperature. The reason is the combined effect of insolation through the polycarbonate sheets (greenhouse effect) and the heat generated by the spectators.
- During the concerts, the mean radiant temperature was approximately equal to the air temperature. This implies that this temperature can be used for thermal comfort assessment of the stadium occupants.
- During the concerts, the water vapor concentration rose to 12-16 g/kg, while the outdoor value was about 7-11 g/kg, indicating a clear impact of the spectator water vapor production.
- During the concerts, the $CO_2$ concentration reached values of about 2000 ppm, while before the concert (unoccupied stadium) the $CO_2$ concentration was only about 420 ppm. The decay curves of the $CO_2$ concentration, and thus the ACH values, were approximately the same at the four measuring positions. The average ACH value was 0.67 $h^{-1}$. Furthermore, the ACH values on three consecutive evenings were within 8% of the average ACH value for each particular position.

The presented on-site full-scale measurement data, in particular during the three concert evenings, will be used in future studies for validation of CFD models for wind flow, natural ventilation and indoor environmental conditions in buildings.

## 7. Acknowledgements

Twan van Hooff is currently a PhD student funded by both Eindhoven University of Technology in the Netherlands and Fonds Wetenschappelijk Onderzoek (FWO) - Flanders, Belgium (FWO project number: G.0435.08). The FWO Flanders supports and stimulates fundamental research in Flanders. Its contribution is gratefully acknowledged.

The measurements reported in this paper were supported by the Laboratory of the Unit Building Physics and Systems (BPS) at Eindhoven University of Technology. Special thanks go to Jan Diepens, head of LBPS, and Wout van Bommel, Harrie Smulders and Geert-Jan Maas, members of the LBPS, for their valuable contributions. The KNMI (Royal Meteorological Institute of the Netherlands) is gratefully acknowledged for providing the wind speed measurement data at Schiphol airport meteorological station.

## 8. References

ASHRAE, 2005. Handbook of Fundamentals. American Society of Heating, Refrigerating and Air-Conditioning Engineers, Inc., Atlanta, USA.

Awbi, H.B., 2007. Ventilation systems: design and performance. London: Taylor & Francis.

Bejan, A., 1984. Convection heat transfer. New York: John Wiley & Sons.

Blocken, B., Carmeliet, J., 2005. High-resolution wind-driven rain measurements on a low-rise building - experimental data for model development and model validation. J. Wind Eng. Ind. Aerodyn. 93, 905–928.

Blocken, B., Janssen, W.D., van Hooff, T., 2012. CFD simulation for pedestrian wind comfort and wind safety in urban areas: General decision framework and case study for the Eindhoven University campus. Environ. Modell. Soft. 30: 15-34.

Blocken, B., Persoon, J., 2009. Pedestrian wind comfort around a large football stadium in an urban environment: CFD simulation, validation and application of the new Dutch wind nuisance standard. J. Wind Eng. Ind. Aerodyn. 97, 255-270.

Blocken, B., Stathopoulos, T., Carmeliet, J., Hensen, J.L.M., 2011. Application of CFD in building performance simulation for the outdoor environment: an overview. J. Build. Perform. Simul. 4(2): 157-184.

Blocken B, Gualtieri C. 2012. Ten iterative steps for model development and evaluation applied to Computational Fluid Dynamics for Environmental Fluid Mechanics. Environ. Modell. Software. In press.

Casey, M., Wintergerste, T. (Eds) 2000. Best Practice Guidelines, ERCOFTAC Special Interest Group on Quality and Trust in Industrial CFD, ERCOFTAC, Triomflaan 43, B-1160, Brussels.

Chen, Q., 2009. Ventilation performance prediction for buildings: A method overview and recent applications. Build. Environ. 44, 848-858.

Dalgliesh, W.A., Surry, D., 2003. BLWT, CFD and HAM modelling vs. the real world: Bridging the gaps with full-scale measurements. J. Wind Eng. Ind. Aerodyn. 91, 1651-1669.

ECA: European Collaborative Action on Urban Air, Indoor Environment and Human Exposure, 1992. Report No. 11: Guidelines for Ventilation Requirements in Buildings, EUR 14449 EN, Luxembourg 1992.

Evola, G., Popov, V., 2006. Computational analysis of wind driven natural ventilation in buildings. Energy Build. 38, 491-501.

Franke, J., Hirsch, C., Jensen, A.G., Krüs, H.W., Schatzmann, M., Westbury, P.S., Miles, S.D., Wisse, J.A., Wright, N.G., 2004. “Recommendations on the use of CFD in wind engineering”. In: van Beeck, J.P.A.J. (Eds.), Proceedings of the International Conference on Urban Wind Engineering and Building Aerodynamics. COST Action C14, Impact of Wind and Storm on City Life Built Environment. Von Karman Institute, Sint-Genesius-Rode, Belgium, 5–7 May 2004.

Franke, J., Hellsten, A., Schlünzen, H., Carissimo, B. (Eds.), Best practice guideline for the CFD simulation of flows in the urban environment. COST Office Brussels, ISBN 3-00-018312-4, 2007.

Heiselberg, P., Li, Y., Andersen, A., Bjerre, M., Chen, Z., 2004. Experimental and CFD evidence of multiple solutions in a naturally ventilated building. Indoor Air 14, 43–54.

Holford, J.M., Hunt, G.R., 2003. Fundamental atrium design for natural ventilation. Build. Environ.38(3), 409-426.

Hu, C.H., Ohba, M., Yoshie, R., 2008. CFD modelling of unsteady cross ventilation flows using LES. J Wind Eng Ind Aerodyn 96,1692-1706.

Hunt, G.R., Linden, P.F, 1999. The fluid mechanics of natural ventilation – displacement ventilation by buoyancy-driven flows assisted by wind. Build Environ. 34, 707–720.

Jiang, Y., Chen, Q., 2002. Effect of fluctuating wind direction on cross natural ventilation in buildings from large eddy simulation. Build Environ 37, 379-386.

Jiang, Y., Alexander, D., Jenkins, H., Arthur, R., Chen, Q., 2003. Natural ventilation in buildings: Measurement in a wind tunnel and numerical simulation with large-eddy simulation. J. Wind Eng. Ind. Aerodyn. 91(3), 331-353.

Karava, P., Stathopoulos, T., Athienitis, A.K., 2007. Wind-induced natural ventilation analysis. Solar Energy 81, 20-30.

Karava, P., Stathopoulos, T., Athienitis, A.K., 2011. Airflow assessment in cross-ventilated buildings with operable façade elements. Build. Environ.46, 266-279.Kato, S., Murakami, S., Mochida, A., Akabayashi,

A., Tominaga, Y., 1992. Velocity-pressure field of cross ventilation with open windows analyzed by wind tunnel and numerical simulation. J. Wind Eng. Ind. Aerodyn. 44, 2575-2586,
Kato, S., Murakami, S., Mochida, A., Akabayashi, S., Tominaga, Y., 1992. Velocity-pressure field of cross ventilation with open windows analyzed by wind tunnel and numerical simulation. J. Wind Eng. Ind. Aerodyn. 44, 2575-86.
Kipp and Zonen 2000. Instruction manual for Kipp & Zonen CM11/CM14 pyranometer/albedometer. Delft, the Netherlands; 2000.
Kobayashi, T., Sandberg, M., Kotani, H., Claesson, L., 2010. Experimental investigation and CFD analysis of cross-ventilated flow through single room detached house model. Build. Environ. 45, 2723-2734.
Kovar-Panskus, A., Moulinneuf, L., Savory, E., Abdelqari, A., Sini, J.-F., Rosant, J.-M., Robins, A., Toy, N., 2002. A wind tunnel investigation of the influence of solar-induced wall-heating on the flow regime within a simulated urban street canyon. Water Air Soil Pollut. Focus 2(5), 555-571.
Lagus, P., Persily, A.K., 1985. A review of tracer-gas techniques for measuring airflows in buildings. ASHRAE Trans. 91(2B), 1075.
Li, Y.G., Delsante, A., 2001. Natural ventilation induced by combined wind and thermal forces. Build Environ. 36, 59–71.
Linden, P.F., 1999. The fluid mechanics of natural ventilation. Annu. Rev. Fluid Mech. 31, 201–238.
Liu, P.-C., Lin, H.-T., Chou, J.-H., 2009. Evaluation of buoyancy-driven ventilation in atrium buildings using computational fluid dynamics and reduced-scale air model. Build. Environ.44(9), 1970-1979.
McIntyre, D.A., 1980. Indoor climate. Applied Science Publishers Ltd, London.
Mochida, A., Yoshino, H., Miyauchi, S., Mitamura, T., 2006. Total analysis of cooling effects of cross-ventilation affected by microclimate around a building. Sol. Energy. 80, 371-382.
Norton, T., Grant, J., Fallon, R., Sun, D.W., 2010. Optimising the ventilation configuration of naturally ventilated livestock buildings for improved indoor environmental homogeneity. Build. Environ. 45, 983-995.
Ohba, M., Irie, K., Kurabuchi, T., 2001. Study on airflow characteristics inside and outside a cross-ventilation model, and ventilation flow rates using wind tunnel experiments. J. Wind Eng. Ind. Aerodyn. 89(14-15), 1513-1524.
Ramponi, R., Blocken, B., 2012a. CFD simulation of cross-ventilation for a generic isolated building: impact of computational parameters. Build. Environ. 53, 34-48.
Ramponi, R., Blocken, B., 2012b. CFD simulation of cross-ventilation flow for different isolated building configurations: validation with wind tunnel measurements and analysis of physical and numerical diffusion effects. J. Wind Eng. Ind. Aerodyn. In press. This issue.
Richards, K., Schatzmann, M., Leitl, B., 2006. Wind tunnel experiments modelling the thermal effects within the vicinity of a single block building with leeward wall heating. J. Wind Eng. Ind. Aerodyn. 94(8), 621-636.
Ruck, B., 1993. Wind-tunnel measurements of flow field characteristics around a heated model building. J. Wind Eng. Ind. Aerodyn. 50, 139-152.
Schatzmann, M., Leitl, B., 2011. Issues with validation of urban flow and dispersion CFD models. J. Wind Eng. Ind. Aerodyn. 99, 169-186
Schatzmann, M., Rafailidis, S., Pavageau, M., 1997. Some remarks on the validation of small-scale dispersion models with field and laboratory data. J. Wind Eng. Ind. Aerodyn. 67&68. 885-893.
Sherman, M.H., 1990. Tracer gas techniques for measuring ventilation in a single zone. Build. Environ. 25(4), 365-374.
Straw, M.P., Baker, C.J., Robertson, A.P., 2000. Experimental measurements and computations of the wind-induced ventilation of a cubic structure. J. Wind Eng. Ind. Aerodyn. 88(2-3), 213-230.
Tominaga, Y., Mochida, A., Yoshie, R., Kataoka, H., Nozu, T., Yoshikawa, M., Shirasawa, T., 2008. AIJ guidelines for practical applications of CFD to pedestrian wind environment around buildings. J. Wind Eng. Ind. Aerodyn. 96(10-11), 1749-1761.
van Hooff, T., Blocken, B., 2010a. Coupled urban wind flow and indoor natural ventilation modelling on a high-resolution grid: A case study for the Amsterdam ArenA stadium. Environ. Modell. Software 25, 51-65.
van Hooff, T., Blocken, B., 2010b. On the effect of wind direction and urban surroundings on natural ventilation of a large semi-enclosed stadium. Comput. Fluids 39, 1146-1155
Wieringa, J., 1992. Updating the Davenport roughness classification. J. Wind Eng. Ind. Aerodyn. 41(1), 357-368.
World Meteorological Organization, 2008. Guide to Meteorological Instruments and Methods of Observation, Appendix 4B, WMO-No. 8 (CIMO Guide), Geneva 2008.

Table 1: Calculated ACH values based on the $CO_2$ concentration decay curves.

| | ACH [$h^{-1}$] | | | |
|---|---|---|---|---|
| | June 1-2 | June 2-3 | June 3-4 | Average |
| N1 | 0.70 | 0.60 | 0.63 | 0.65 |
| N2 | 0.70 | 0.75 | 0.76 | 0.74 |
| SE1 | 0.64 | 0.74 | - | 0.69 |
| SE2 | 0.64 | 0.62 | 0.58 | 0.61 |

FIGURE CAPTIONS

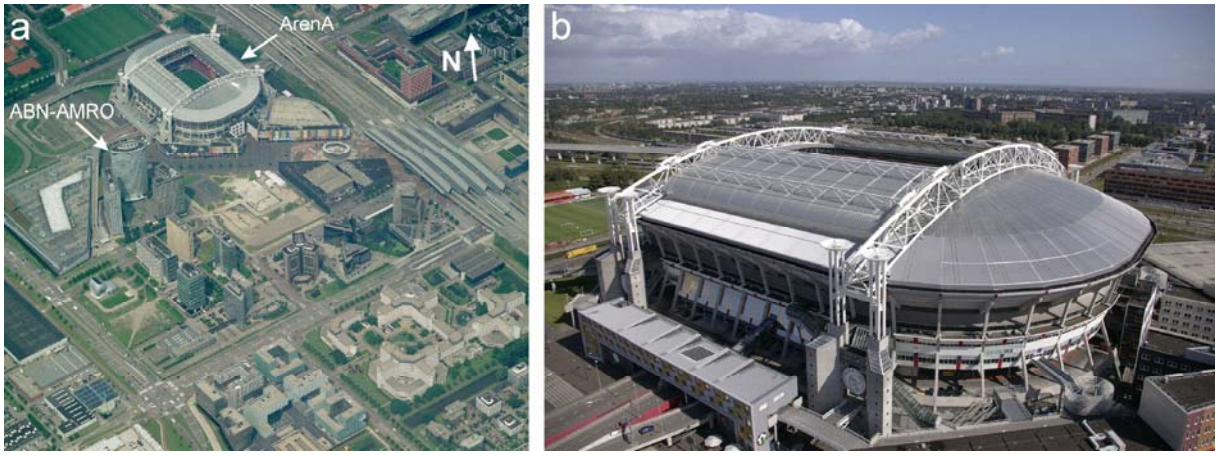


Fig. 1: (a) Aerial view of the ArenA and its surroundings, including the ABN-AMRO office tower building. (b) Picture of the stadium taken from the ABN-AMRO office tower.

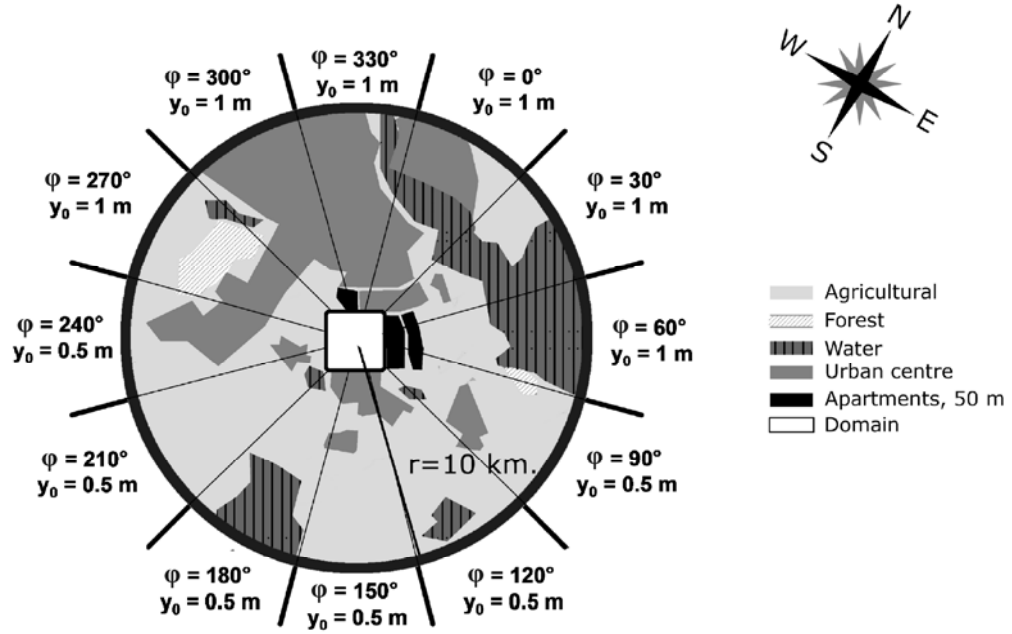


Fig.2: Terrain surrounding the stadium with a radius of 10 km and estimated aerodynamic roughness length $y_0$ based on an upstream distance of 10 km. The white square represents the area of interest, shown in Fig. 1a.

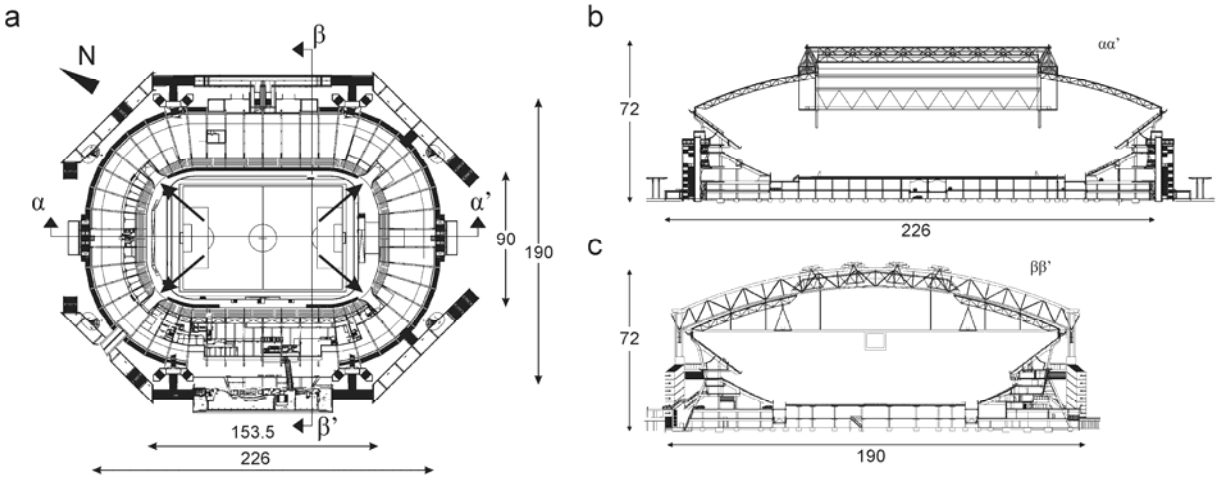


Fig. 3: (a) Horizontal cross-section of stadium. The arrows indicate the four large openings (gates) in the corners of the stadium (see Fig. 4b). (b) Vertical cross-section αα'; (c) cross-section ββ'. Dimensions in m.

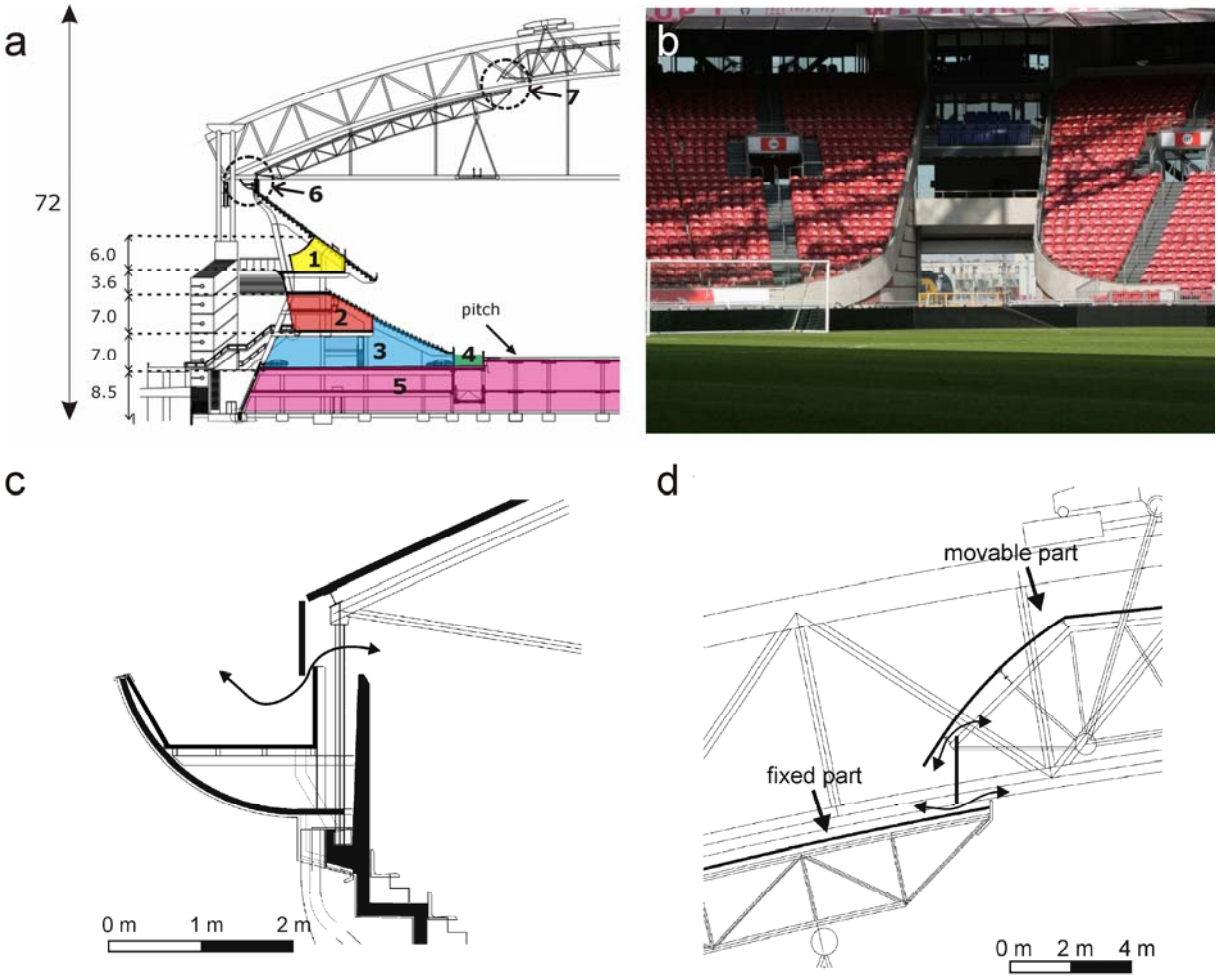


Fig. 4: (a) Vertical cross-section of the stadium illustrating the different components of the stadium. (b) Opening (gate) in the corner of the stadium (41.5 $m^2$). (c) Ventilation opening between the stand and the steel roof construction (130 $m^2$). (d) Ventilation opening between the fixed and movable part of the roof (85 $m^2$). Dimensions in m.

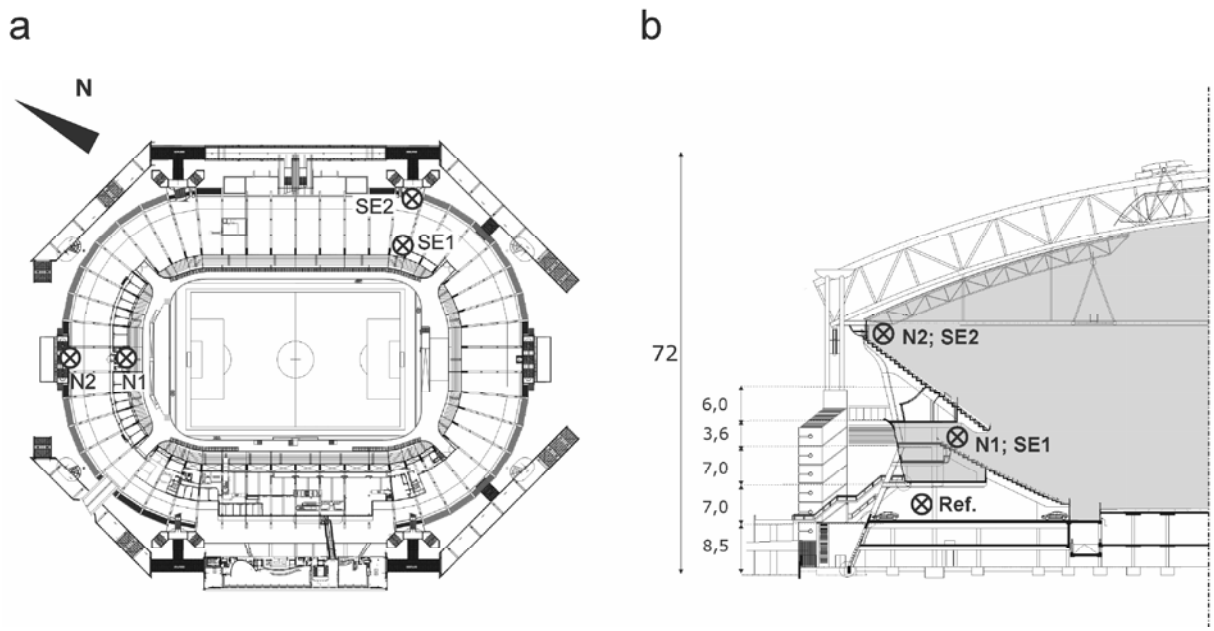


Fig. 5: (a) The four indoor measurement positions (⊗) in stadium plan view. (b) The four indoor measurement positions and the outdoor reference position in a vertical cross-sectional view. The grey area indicates the stadium interior volume.

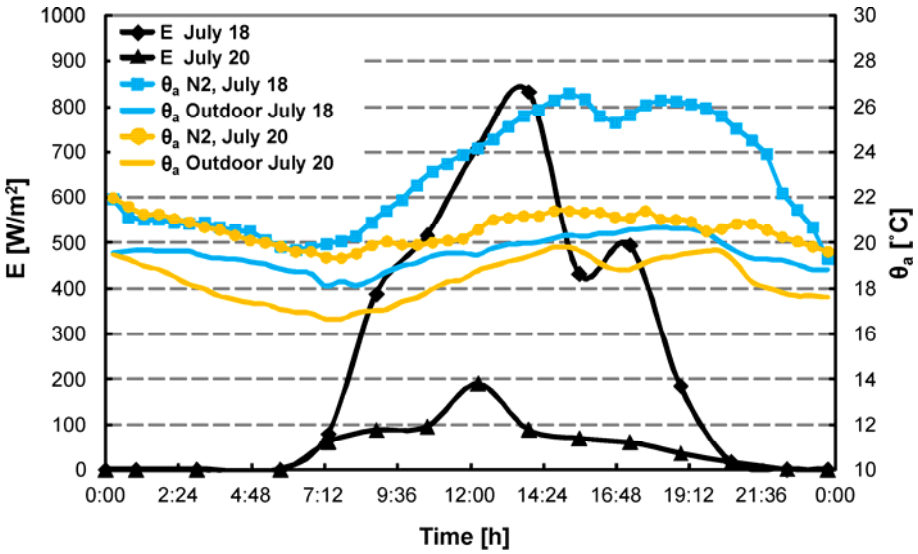


Fig. 6: Measurements of outdoor irradiance (E), outdoor air temperature and indoor air temperature ($\theta_a$) at position N2 on a sunny day (July 18) and a cloudy day (July 20).

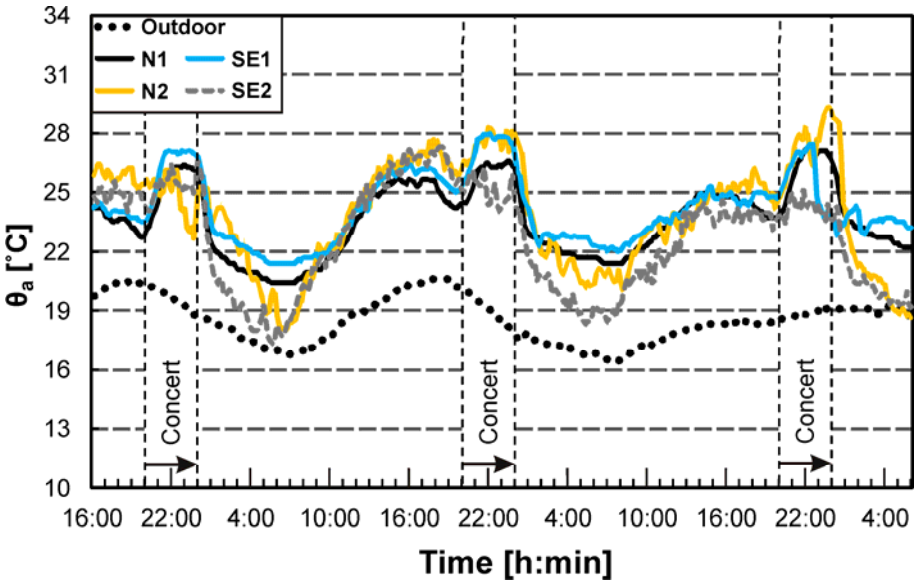


Fig. 7: Measured outdoor and indoor air temperature ($\theta_a$) from the afternoon of June 1 until the early morning of June 4, 2007. The dashed vertical lines indicate the beginning and the end of a concert in the stadium.

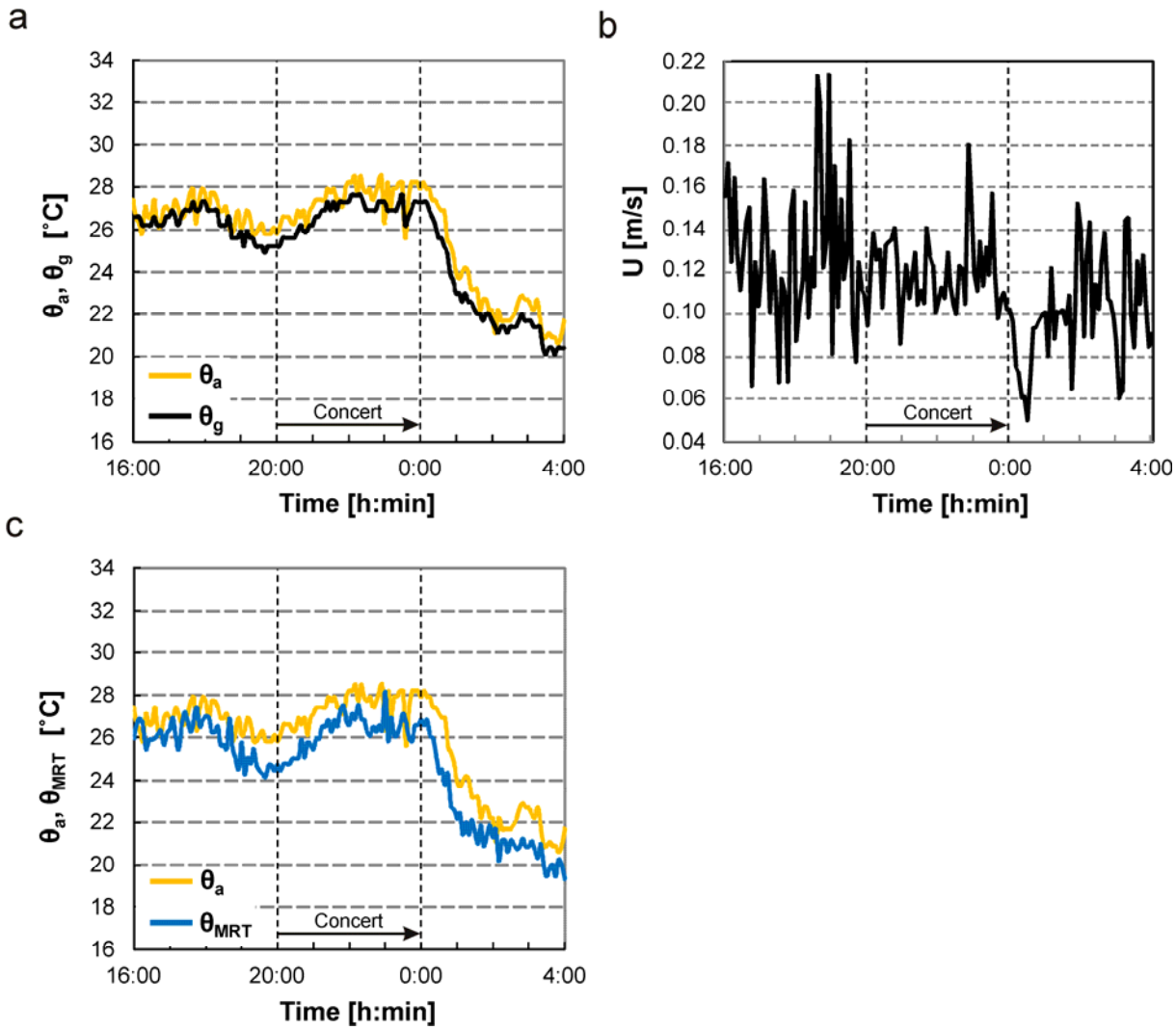


Fig. 8: (a) Measured air temperature ($\theta_a$) and globe temperature ($\theta_g$) at position N2 on June 2-3, 2007. (b) Measured air temperature ($\theta_a$) and mean radiant temperature ($\theta_{MRT}$) at position N2 on June 2-3, 2007. (c) Measured indoor air speed at position N2 on June 2-3, 2007.

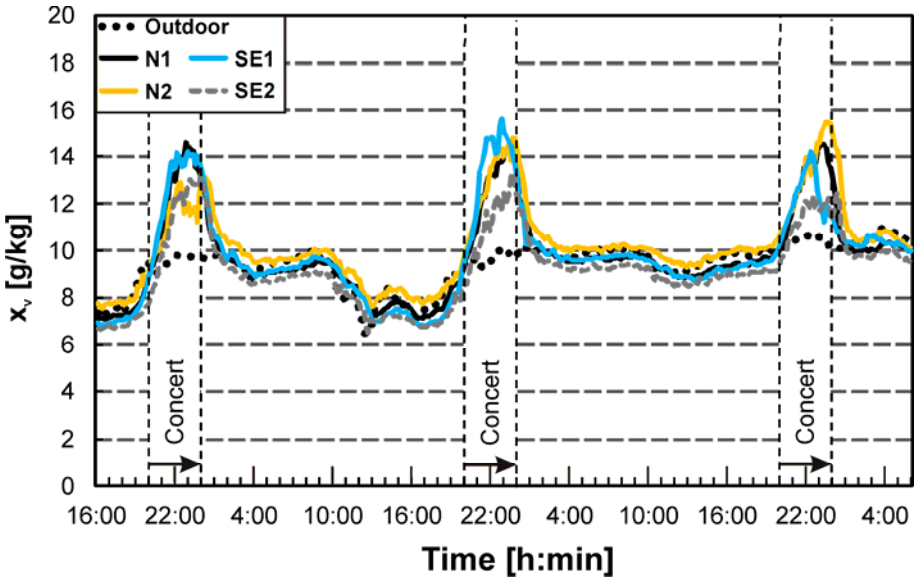


Fig. 9: Measured outdoor and indoor water vapor concentration ($x_v$) from the afternoon of June 1 until the early morning of June 4, 2007. The dashed vertical lines indicate the beginning and the end of a concert in the stadium.

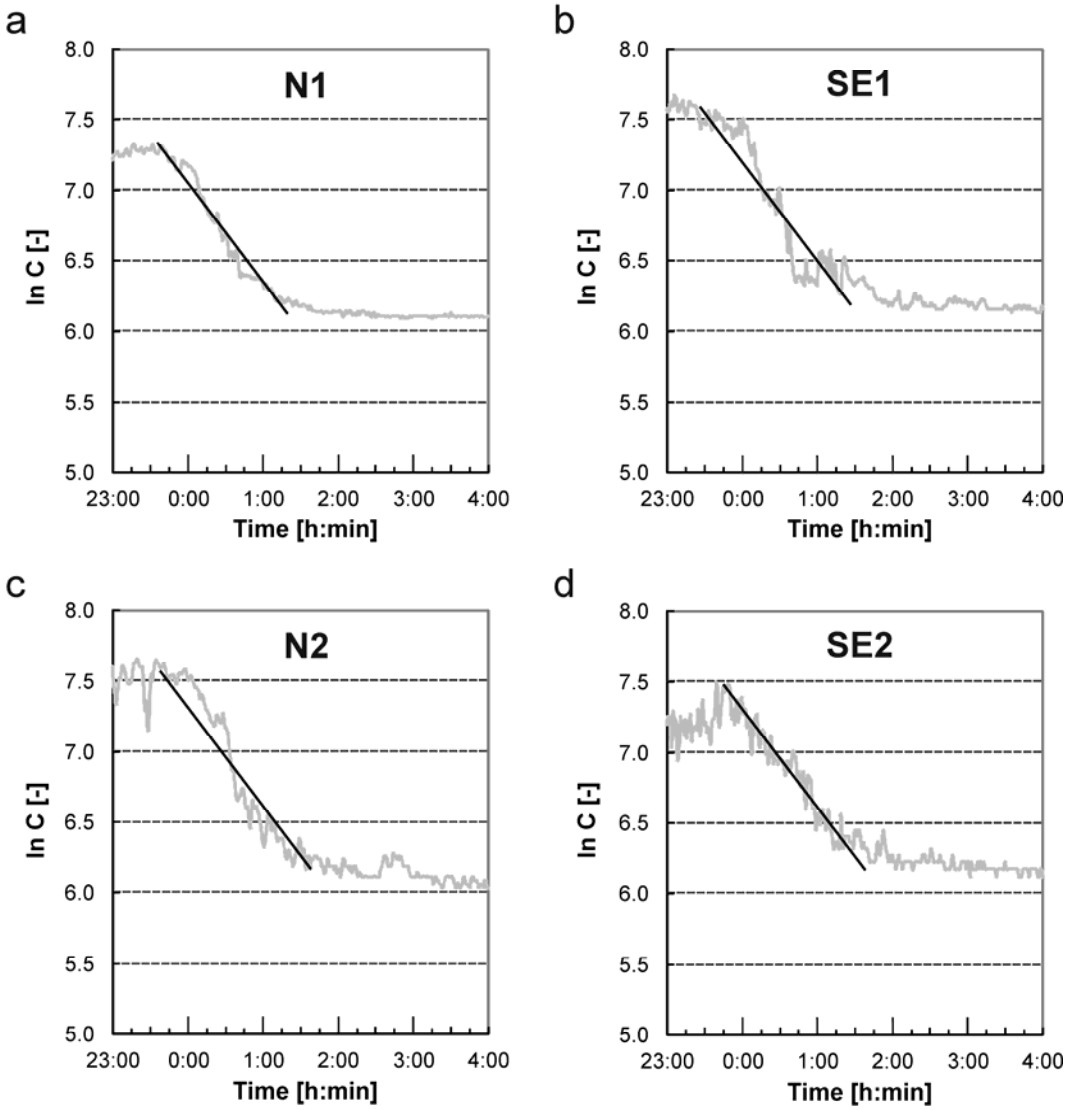


Fig. 10: $CO_2$ concentration decay curves at the four indoor measurement positions on June 2-3, 2007. (a) N1; (b) SE1; (c) N2; (d) SE2.

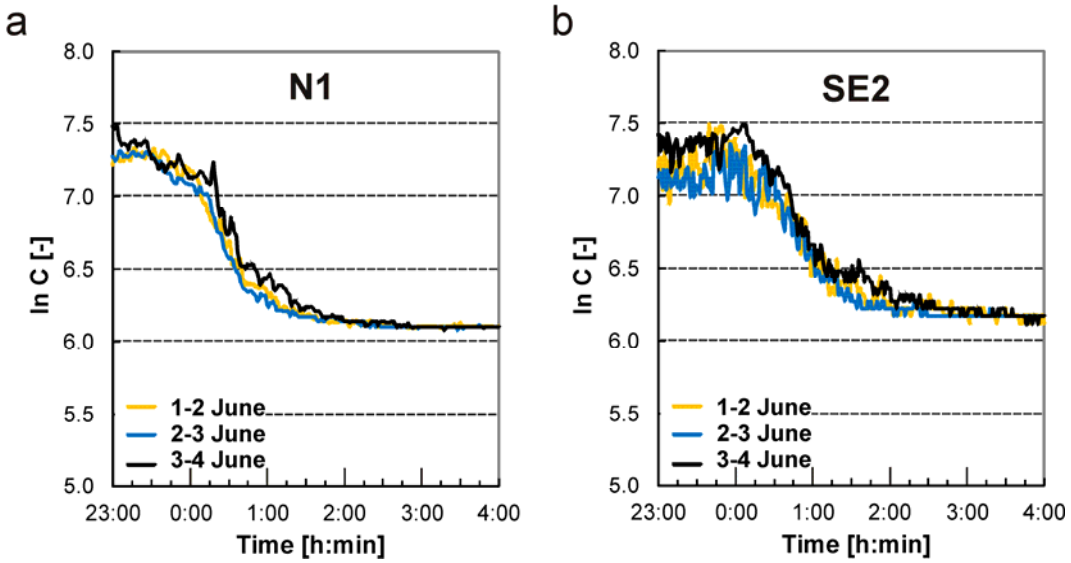


Fig. 11: $CO_2$ concentration decay curves on three consecutive evenings/nights (June 1-2, June 2-3, June 3-4, 2007) at two positions. (a) N1; (b) SE2.

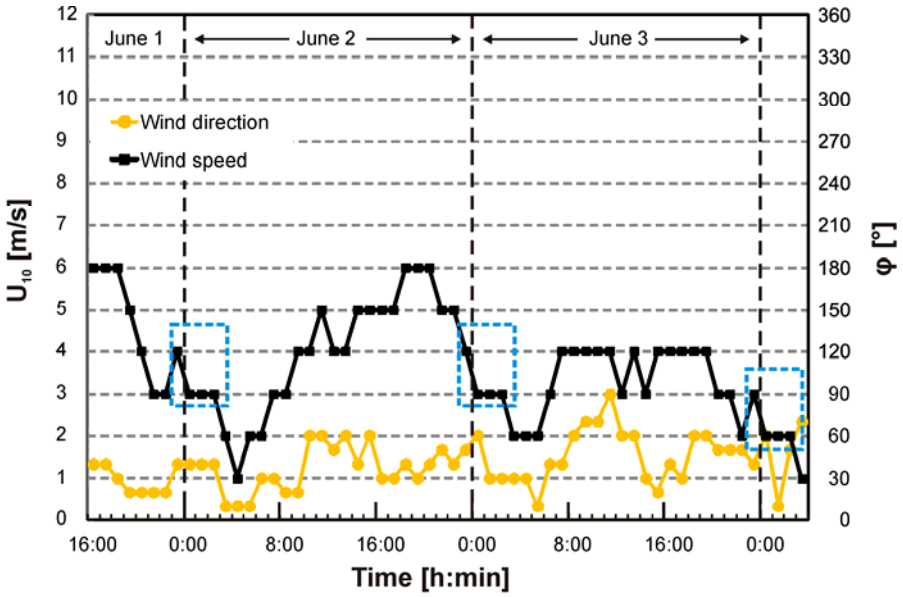


Fig. 12: Measured reference wind speed and wind direction from the afternoon of June 1 until the early morning of June 4, 2007, at the meteorological station of the KNMI at Schiphol. The dashed squares roughly indicate the periods during which the $CO_2$ concentration decay measurements were performed.